Animal Reproduction Science 200 (2019) 86–95

Contents lists available at ScienceDirect

Animal Reproduction Science

journal homepage: www.elsevier.com/locate/anireprosci

Bmp4 inhibits goose granulosa cell apoptosis *via* PI3K/AKT/Caspase-9 signaling pathway

Junsong Yuan[1], Yan Deng[1], Yingying Zhang, Xiang Gan, Shanyan Gao, Hang Hu, Shenqiang Hu, Jiwei Hu, Hehe Liu, Liang Li, Jiwen Wang*

Farm Animal Genetic Resources Exploration and Innovation Key Laboratory of Sichuan Province, Sichuan Agricultural University, Chengdu, Sichuan, 611130, PR China

ARTICLE INFO

Keywords:
Geese
BMP4
Granulosa cells
Apoptosis
PI3K/AKT/Caspase-9

ABSTRACT

Bone morphogenetic protein 4 (BMP4) has an important role in regulating cellular proliferation, differentiation and apoptosis. It, however, is still unclear as to the mechanisms by which *BMP4* regulates the apoptosis of granulosa cells (GCs) in geese. In the present study, there was cloning of the full-length coding sequence of goose *BMP4* gene, which consisted of 1212 nucleotides encoding 403 amino acids. Its deduced amino acid sequence comprised one signal peptide, one TGFβ pro-peptide and one mature peptide domain. Results from conducting the quantitative real-time PCR (qPCR) indicated the relative abundances of *BMP4* mRNA in geese GCs increased gradually from the relative abundances in pre-hierarchical follicles that were 4 to 6 mm in diameter to that in the fifth largest (F5) follicle and then relative abundances of *BMP4* mRNA decreased with further development as the largest (F1) follicle. Results from use of the TUNEL assay indicated that overexpression of the goose *BMP4* gene suppressed GC apoptosis and this was confirmed when relative abundances of the CAD, Caspase-9 and Caspase-3 proteins were determined using western blotting. In addition, overexpression of the *BMP4* gene induced phosphorylation of AKT, which was inhibited with use of the PI3K inhibitor, LY294002. Co-transfection of *BMP4* and LY294002 resulted in increased relative abundances of Caspase-9 and CAD proteins but had no effect on that of Caspase-3. Taken together, these results suggested that expression of the *BMP4* gene resulted in a reduction in Caspase-9 protein leading to inhibition of GC apoptosis via the PI3K/AKT signaling pathway in geese.

1. Introduction

Granulosa cells (GCs), located between the oocyte and peripheral theca cells (TCs) in ovarian follicle, are essential for follicular development and maturation. The primary factor in follicle atresia is apoptosis of the GCs (Tilly et al., 1991; Inoue et al., 2011), which occurs as a result of complex interactions between numerous extra- and intra-ovarian factors (Johnson, 2003). Among ovarian-produced growth factors, the transforming growth factor β (TGFβ) superfamily was reported to have important roles in regulation of ovarian functions in chickens (Onagbesan et al., 2003).

Bone morphogenetic protein 4 (BMP4), as a member of the TGFβ superfamily, has been reported to be involved in regulation of mammalian ovarian folliculogenesis (Knight and Glister, 2006). In previous studies, there has been examination of the abundance of

* Corresponding author.
E-mail address: wjw2886166@163.com (J. Wang).
[1] These authors contributed equally to this study.

https://doi.org/10.1016/j.anireprosci.2018.11.014
Received 21 July 2018; Received in revised form 29 October 2018; Accepted 30 November 2018
Available online 01 December 2018
0378-4320/

BMP4 mRNA in ovarian follicular cells of sheep (Bertoldo et al., 2014), cattle (Fatehi et al., 2005; Da et al., 2017), mice (Ding et al., 2013), rats (Nilsson and Skinner, 2003) and chickens (Onagbesan et al., 2003). In mammals, *BMP4* could function as a paracrine factor to promote the development of follicles (Shimasaki et al., 1999). Studies in mice indicated that *BMP4* could not only decrease the rate of primordial follicle atresia through suppressing the apoptosis of oocytes (Ding et al., 2013). Furthermore, it had also been reported that relative abundance of *BMP4* was related to GC apoptosis during follicle development (Shimasaki et al., 2004). Although the GCs had a lesser rate of apoptosis in cattle, *BMP4* treatment did not affect the relative abundance of mRNA of apoptotic-related genes (Kayamori et al., 2008). This finding implied that *BMP4* might regulate the GC apoptosis through other pathways. One function of *BMP4* is to inhibit the nuclear transfer of caspase-actived Dnase (CAD) protein in GCs of cattle, and the activation of CAD required caspase-3-dependent proteolysis of CAD inhibitor (ICAD) (Lechardeur et al., 2005; Kayamori et al., 2008). These results indicated that *BMP4* might directly inhibit the activity of CAD by stimulating caspase-3 activity in regulation of GC apoptosis. It has been reported that *BMP4* inhibited apoptosis of GCs via the PI3K/PDK-1/AKT signaling pathway in cattle (Shimizu et al., 2012). Furthermore, *BMP4* also inhibited oocyte apoptosis and, therefore, was involved in regulation of follicular growth by the BMPs/SMADS classical signaling pathway (Shi and Massague, 2003; Drummond, 2005; Koinuma et al., 2005; Ding et al., 2013; Zhang et al., 2015). These data suggested that *BMP4* regulated the GC apoptosis through multiple signaling pathways. At present, the relative abundances of *BMP4* mRNA in hen GCs were increased with follicular development from the pre-hierarchical stage when follicles were 3 to 5 mm in diameter to the time these follicles developed to be the fifth largest (F5) follicle (Kim et al., 2013). There was also a progressive increase during the development of the third largest (F3) to the first largest (F1) follicle (Onagbesan et al., 2003). The regulatory mechanisms are not understood for the *BMP4* gene expression that controls amount of BMP4 transcript produced and ultimately abundance of *BMP4* protein in geese follicle development.

The present study, therefore, focused on cloning the complete coding sequence of the goose *BMP4* gene followed by bioinformatic analysis, determination of relative abundance of mRNA in follicles at different developmental stages, and elucidation of the mechanisms by which *BMP4* regulates apoptosis of GCs. These results will help broaden the understanding of the role of *BMP4* in geese ovaries as well as its regulatory mechanisms in follicle development.

2. Materials and methods

2.1. Animals and sample collection

The Sichuan White Geese (*Anser cygnoide*) used in this study were 34 to 36 weeks of age, had free access to water, and was maintained in natural lighting and temperature conditions at the Waterfowl Breeding Experimental Farm of Sichuan Agricultural University (Sichuan, China). Three geese were used for determining the relative abundance of *BMP4* mRNA in GCs of different sized follicles and six geese were used for collection of GCs for *in vitro* culturing. Ovarian follicles were dissected from each goose and subsequently washed with ice-cold sterile phosphate buffered saline (PBS, pH = 7.4, Solarbio). Follicles were classified into pre-hierarchical (4–6 mm, 6–8 mm, 8–10 mm) and hierarchical (from the fifth to the largest follicle (F5-F1)) follicles according to diameter (Wei et al., 2013). The granulosa layers of follicles were isolated using previously reported procedures (Deng et al., 2018). The isolated granulosa layers were frozen in liquid nitrogen until RNA extraction. All procedures in the present study were approved by the Institutional Animal Care and Use Committee (IACUC) of Sichuan Agricultural University (Permit No. DKY-B20141401).

2.2. RNA extraction and molecular cloning

Total RNA was isolated from granulosa layers of different sized follicles using TRIzol (Takara, Japan). The purity and quality of total RNA were assessed by spectrophotometric absorbance at 260/280 nm and 260/230 nm, respectively. The integrity of RNA was assessed with use of an agarose gel. Complementary DNA (cDNA) was synthesized from 1 μg of total RNA using a cDNA synthesis kit (Takara, Japan) according to the manufacturer's instruction. The PCR was performed using a program that resulted in a 95 ℃ pre-denaturing for 10 min, followed by 35 cycles of 30 s at 95 ℃, primer-specific annealing temperature for 30 s, 72 ℃ for 1 min 30 s which was subsequently followed by a final extension for 10 min at 72 ℃. The PCR products were gel-purified using a gel extraction kit (Omega Bio-Tek, Norcross, Georgia, USA). Target cDNA was ligated into the pMD-19 T vector (Takara, Japan) and was then transformed into *E. coli* DH5α competent cells. Positive clones that contained the expected-size inserts were screened by using colony PCR and were then sequenced by using the Qinke procedure (Chengdu, China). Primers of *BMP4* are shown in Table 1.

2.3. Bioinformatical analysis

The BlASTn program on NCBI was used to analyze the accuracy of cloning sequence (https://blast.ncbi.nlm.nih.gov/Blast.cgi). Homology analyses of nucleotide and amino acid sequences were performed using the DNAMAN software. ProScale (https://web.expasy.org/protscale/) programs were used for predicting the physiochemical properties of the BMP4 protein. The structure domains of amino acid sequence were analyzed using the Conserved Domains Database (CDD, https://www.ncbi.nlm.nih.gov/Structure/cdd/wrpsb.cgi) and SignalIP (http://www.cbs.dtu.dk/services/SignalP/). A phylogenetic tree was calculated using the MEGA 7.0 software by neighbor-joining method and bootstrap replicates with 1000 times.

Table 1
Primer sequences used in the study for *BMP4*.

Primer name	Sequence(5'-3')	Tm(°C)	Size(bp)
RT-PCR			
BMP4	F ATGATTCCTGGTAACCGAATGC R TCAGCGGCACCCGCAC	58	1212
q-PCR			
BMP4	F AAGTGATGAAGCCGCTGTCG R TTGCCCTGATGAGTCTGTGC	60	198
β-actin	F CAACGAGCGGTTCAGGTGT R TGGAGTTGAAGGTGGTCTCG	60	92
18 s	F TTGGTGGAGCGATTTGTC R ATCTCGGGTGGCTGAACG	60	129

F: sense primers; R: antisense primers.

2.4. Quantitative real-time PCR (qPCR)

The relative abundance of *BMP4* mRNA was measured in granulosa layers of different sized follicles by qPCR. The qPCR reactions were performed in a 96-well iQTM5 system (Bio-Rad. USA) using a Takara ExTaq RT-PCR kit and SYBR Green as the detection dye (Takara, Japan). The procedures included 95 ℃ for 30 s, followed by 40 cycles of 95 ℃ for 5 s imposing the annealing temperature for 30 s and at 72 ℃ for 10 min. An 80-cycle melting curve was performed, starting at a temperature of 65 ℃ and increasing by 0.5 ℃ every 10 s to determine primer specificity. Each sample was repeated three times and the relative abundances of mRNA for genes were normalized to *β-actin* and *18 s rRNA* using the $2^{-\Delta\Delta Ct}$ method (Livak and Schmittgen, 2001). Primers designed for qPCR are shown in Table 1.

2.5. Culture of GCs

The GCs of pre-hierarchical follicles were used to investigate the apoptosis of GCs according to the relative abundance profiles of *BMP4* mRNA during follicle development. The cells were cultured for 48 h to treat *in vitro* considering the growth characteristics of GCs that were previously reported (Deng et al., 2018). The culture medium was replaced every 24 h and it included Dulbecco's Modified Eagle's Medium/Nutrient Mixture (DMEM/F12), 10% Fetal Bovine Serum (FBS, Gibco), and 1% streptomycin and penicillin mixture (Gibco). Cells were incubated at 37 ℃ in 5% CO_2-humidified atmosphere to reach 50% confluence for transfection. The cells were seeded on 6-well plates for the TUNEL assay and protein collection, on 12-well plates for RNA extraction and on 96-well plates for the 3-(4,5-Dimethylthiazol-2-yl) -2,5-diphenyltetrazolium bromide (MTT) assay.

2.6. Construction of BMP4 overexpression vector and transient transfection

The coding sequence (CDS) of the goose *BMP4* gene was inserted into the pEGFP-N1 plasmid via Xho I and EcoR I sites. After sequencing by Qinke (Chengdu, China), the recombinant plasmid was confirmed and termed pEGFP-N1-BMP4. To evaluate its quality, the recombinant plasmid was extracted and double digested by Xho I and EcoR I. The pEGFP-N1 (Control), pEGFP-N1-BMP4, LY294002 (an inhibitor of PI3K/AKT signaling pathway), pEGFP-N1-BMP4 + LY294002 respectively were transfected into GCs using lipofectamine® 3000 (Thermofisher, USA) using the manufacturer's protocol. The steps of transfection were as follows: initially, the different plasmids and lipofectamine® 3000 were diluted, respectively, with serum-free DMEM without antibiotics. The diluted lipofectamine® 3000 was subsequently added into each diluted plasmid (1:1 ratio) separately to form oligonucleotide-lipofectamine® 3000 complexes. Next, the complexes were incubated for 5–10 min at room temperature. After transfection, cells were harvested for MTT, TUNEL, qPCR and western blotting experiments. The pEGFP-N1-BMP4 plasmid or the pEGFP-N1 plasmid were transfected into 12- well plates for 24 h for conducting the qPCR experiment and 6- well plates for 48 h for the TUNEL experiment. For western blotting experiment, pEGFP-N1-BMP4 plasmid, LY294002 and pEGFP-N1-BMP4 + LY294002 were, respectively, transfected into 6-well plates for 48 h. For the MTT experiment, LY294002 was transfected into 96-well plates for 24 h according to the previously described methods (Deng et al., 2018).

2.7. TUNEL assay

After transfection for 48 h, the apoptotic cells were detected using the TdT-mediated dUTP nick-end labeling (One Step TUNEL Apoptosis Assay Kit, Beyotime Biotech, China) method (Gavrieli et al., 1992). Briefly, the medium was discarded and GCs were washed with PBS. Then, GCs were fixed by 4% paraformaldehyde for 30 min. The GCs were subsequently washed with PBS and incubated with 0.3% Triton X-100 for 5 min at room temperature. The TUNEL mixture (TdT enzyme, fluorescent marking liquid and detection liquid) was made using the manufacturer's protocol. There were 50 μl of the mixture added into samples and incubated for 60 min avoiding light exposure. After incubating, the GCs were washed three times with PBS and fluorescence quenching was used for sealing. Then, 2-(4-Amidinophenyl) -6-indolecarbamidine dihyrdochloride (DAPI, 10 mg/ml in PBS, Beyotime Biotech, China) was added for 5 min to label all nuclei. The cells were subsequently observed using a fluorescence microscope (Nikon, Japan). Each

Table 2
The information of primary and secondary antibody.

Primary antibody	Dilution rate	secondary antibody	Provider	Catalogs
Mouse-monoclonal-anti-BMP4	1:500	FITC-goat anti-mouse IgG	Santa Cruz (USA)	sc-12721
Mouse- polyclonal-anti-GAPDH	1:5000	FITC-goat anti-mouse IgG	TransGen Biotech (China)	HC301-01
Rabbit- polyclonal-anti-p-AKT	1:500	FITC-goat anti-rabbit IgG	Cell Signaling Technology (USA)	4060S
Rabbit- polyclonal-anti-AKT	1:200	FITC-goat anti-rabbit IgG	Bioss (China)	bs-0115R
Mouse-monoclonal-anti-cleaved-Caspase-9	1:500	FITC-goat anti-mouse IgG	Santa Cruz (USA)	NB100-56122SS
Rabbit- polyclonal-anti-cleaved-Caspase-3	1:400	FITC-goat anti-rabbit IgG	Sangon (China)	D260009
Rabbit- polyclonal-anti-CAD	1:200	FITC-goat anti-rabbit IgG	Bioss (China)	bs-0043R

treatment had three replicates.

2.8. Western blotting

The relative abundance of BMP4 protein, phosphorylation of AKT (p-AKT), total AKT (t-AKT), activated- Caspase-9, actived-Caspase-3, CAD (also termed DFFB) were detected by western blotting. Briefly, total proteins of GCs were extracted from GCs using a mixture of Radio Immunoprecipitation Assay (RIPA) lysis buffer and Phenylmethanesulfonyl fluoride (PMSF) (ratio = 1:1000) (Beyotime Biotech, China). The concentrations of total proteins were adjusted using BCA Protein Assay Kit (Beyotime Biotech, China) to 20 μg per well for loading. The concentration of 8% resolving gel was used for these proteins except activated-Caspase-3 using 12% resolving gel. The proteins were transferred onto polyvinylidene difluoride (PVDF) membranes (Solarbio, China) at 200 mA for 90 min and then blocked with 5% (w/v) fat-free milk at room-temperature for 2.5 h. After that, the membranes were incubated with the primary antibody at 4 ℃ for 12 h and the corresponding secondary antibody at 37 ℃ for 1 h. At last, the membranes were detected by using the ECL kit (Bio-Rad, USA) on a ChemiDoc™ MP Imaging System (Bio-Rad, USA). The abundance of GAPDH protein was used for the loading control. Each treatment had three replicates. Information about the antibodies that were used is shown in Table 2.

2.9. Data analysis

Each experiment was conducted in triplicate. The normal distribution and homogeneity of variances of all data were tested with a Shapiro-Wilk test (Shapiro and Wilk, 1965) and Leven's test (Wu and Wong, 2003), respectively. Multiple comparisons were performed using an ANOVA followed by the Turkey's test using SPSS. 24.0. An independent non-paired *t*-test analysis (two-tailed) was used for the comparison between of two groups. All data are presented as the mean ± S.D. *P*-values of less than 0.05 were considered statistically significant.

3. Results

3.1. Cloning and sequence analysis of goose BMP4

After sequencing, the full-length coding sequence of goose BMP4 was obtained (Fig. 1A). The complete coding sequence of goose BMP4 (GenBank accession NO. KJ546433.1) contained 1212 nucleotides encoding 403 amino acids. The molecular weight of amino acids was 45.94 kDa and the theoretical isoelectric point was 9.17. Homology analysis of goose BMP4 suggested there was a high sequence homology with other avian species such as ducks (98.5%) and chickens (98%), an intermediate homology with mammals such as humans (83.4%) and mice (83.7%), and a relatively lesser homology with that of the chameleons (70.4%) and zebrafish (69.8%). The conserved domain analysis indicated the goose BMP4 amino acid sequence contained one signal peptide, one TGFβ pro-peptide and one mature peptide domain (Fig. 1B). Considering the homology of each domain in various species, there were greater homologies (more than 96%) in the mature peptide domain (Fig. 1C), in contrast, there was a relatively lesser conservation (just 79.93%) in the pro-peptide domain (Supplement 1). The predicted seven-cysteine residues were located in the mature peptide domain and in the carboxy-terminal domain of goose BMP4 (Fig. 1A). In addition, a phylogenetic tree was built based on the BMP4 amino acid sequences for geese and other species (Fig. 2), which indicated that the goose BMP4 was similar to BMP4 of Taeniopygia guttata.

3.2. Relative abundance profile of BMP4 mRNA in GCs during follicle development

As depicted in Fig. 3, the relative abundance of *BMP4* mRNA in GCs increased during follicle development and the greatest abundance was detected in F5 follicles with there being a lesser abundance in F4 follicles and there was less in F3 - F1 ($P < 0.05$) than F4 follicles.

3.3. BMP4 inhibits apoptosis of goose GCs

To evaluate the effect of *BMP4* on GC apoptosis from pre-hierarchical follicles, the overexpression plasmid of *BMP4* (1200 ~ 1300

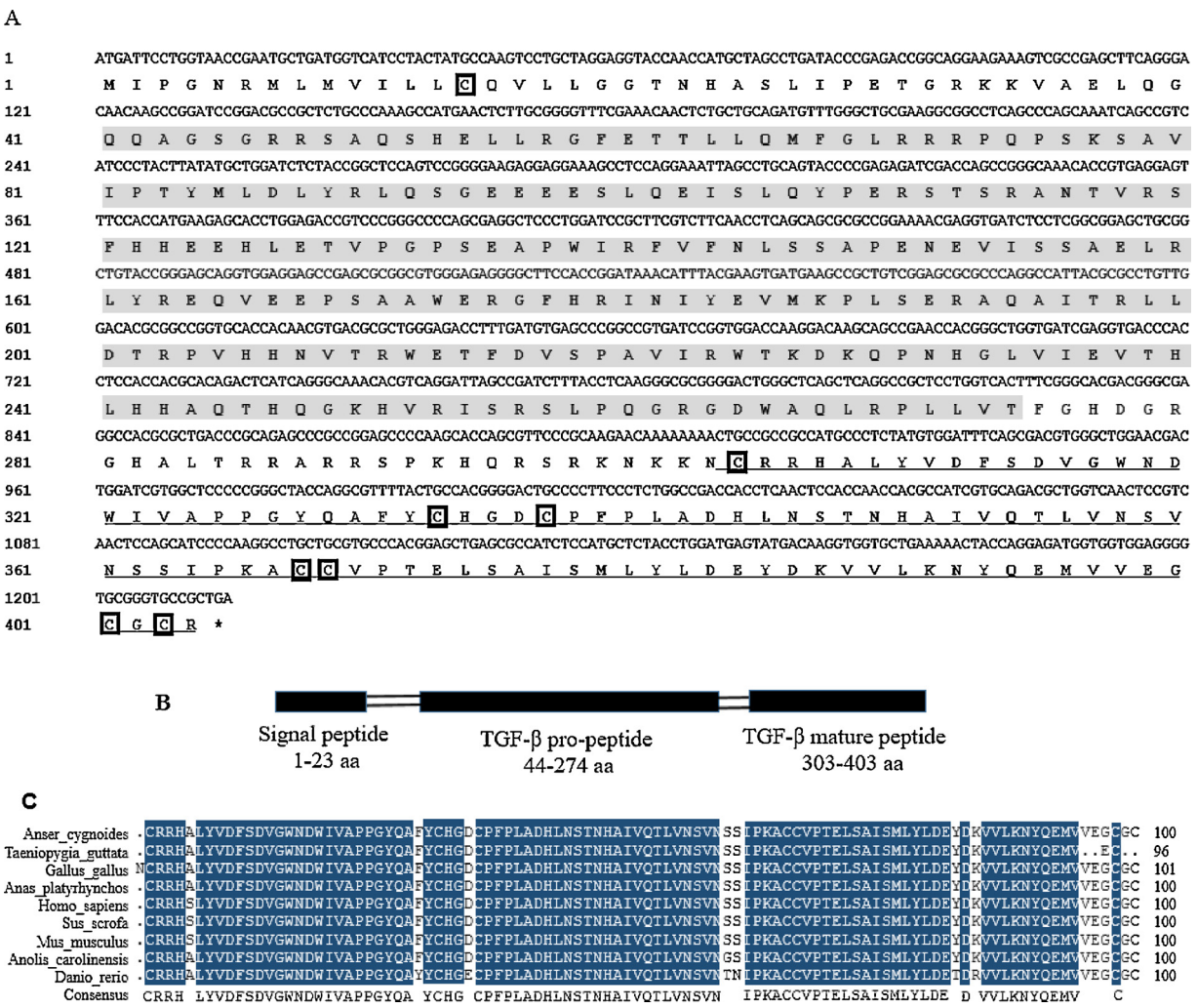

Fig. 1. Nucleotide and amino acid sequences of goose *BMP4* and the predicted structural domains. (A) Nucleotide and amino acids sequences are both numbered on the left side. The entire deduced amino acid sequence is depicted in single letter code beneath the corresponding nucleotide sequence. The stop codon TGA is with '*'. The Cysteine is marked by boxes. The predicted TGF-β pro-peptide domain is marked by '' and TGF-β mature peptide domain is marked by '' . (B) The location of predicted structural domains in the amino acid sequence of goose *BMP4*. The black boxes represent the predicted domains, the double lines represent the rest amino acid sequence. (C) The homology comparison of mature peptide domain among different species. Amino acid sequences are numbered on the right side. The black background represent the consistency of amino acid.

bp) was successfully constructed (Supplement 2) and was transiently transfected into GCs from pre-hierarchical follicles cultured *in vitro*. After 48 h of transfection, the relative abundance of BMP4 protein was greater in pEGFP-N1-BMP4 than in the control (Fig. 4A and B, $P < 0.05$). Results from the TUNEL assay indicated that the apoptotic rate of GCs in pEGFP-N1-BMP4 was less (Fig. 4C and D, $P < 0.05$) as compared with the control. The results using the qPCR indicated that relative abundance of *bcl-2* mRNA was greater while that of *caspase-3* mRNA was relatively less in pEGFP-N1-BMP4 transfected cells as compared with the relative control (supplementary 3 A and 3B, $P < 0.05$). In addition, results from western blotting indicated that the abundances of CAD (Fig. 4A and 4B, $P < 0.05$) and cleaved-Caspase-9, cleaved-Caspase-3 (Fig. 5A and B, $P < 0.05$) protein were less compared with the control while the amount of phosphorylation of AKT (Fig. 5A and B, $P < 0.05$) was greater in pEGFP-N1-BMP4 than in the control.

3.4. There is inhibition of apoptosis in goose GCs by BMP4 via the PI3K/AKT/Caspase-9 signaling pathway

To further explore whether *BMP4* inhibited apoptosis of GCs in pre-hierarchical follicles through the PI3K/AKT/Caspases signaling pathway, the PI3K inhibitor LY294002 was used. The results from the MTT assay indicated that inclusion of LY294002 reduced the viability of GCs in a dose-dependent manner, and 20 μM LY294002 was utilized in subsequent experiments (supplementary 4 A, $P < 0.05$). Compared with pEGFP-N1-BMP4, the amount of AKT phosphorylation was less (Supplementary 4B and 4C, $P < 0.05$), while the abundance of protein for cleaved-Caspase-9, cleaved-Caspase-3 and CAD was greater (Fig. 5A and B, $P < 0.05$) when there was LY294002 transfection. When pEGFP-N1-BMP4 and LY294002 were co-transfected into the GCs, the amount of

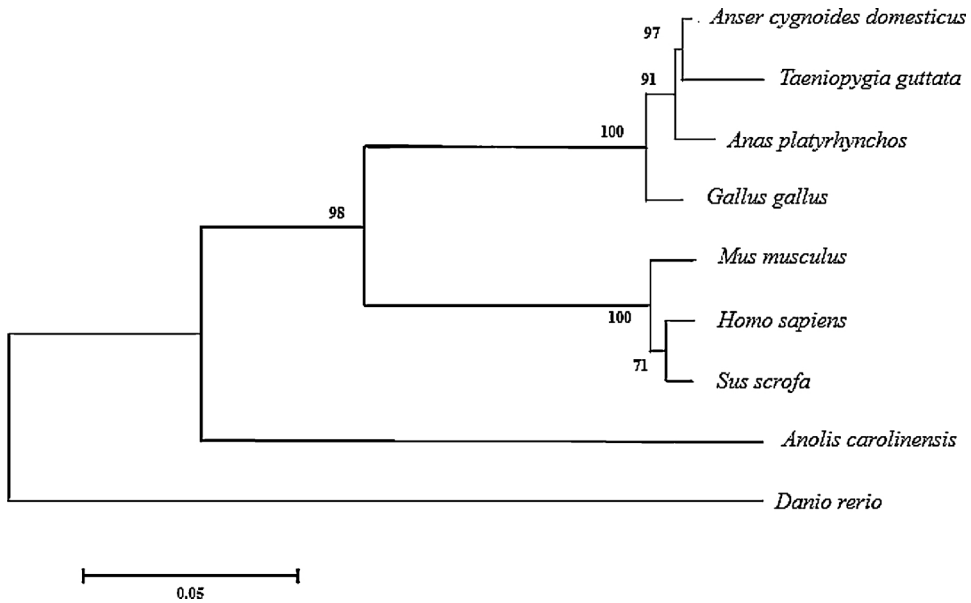

Fig. 2. A phylogenetic tree of goose *BMP4*. The *BMP4* sequences from other species were constructed by using the maximum likelihood method. The bootstrap sampling was performed with 1000 replicates and the numbers at the forks indicate the bootstrap proportions. The scale bar represents the expected number of amino acid substitutions per site.

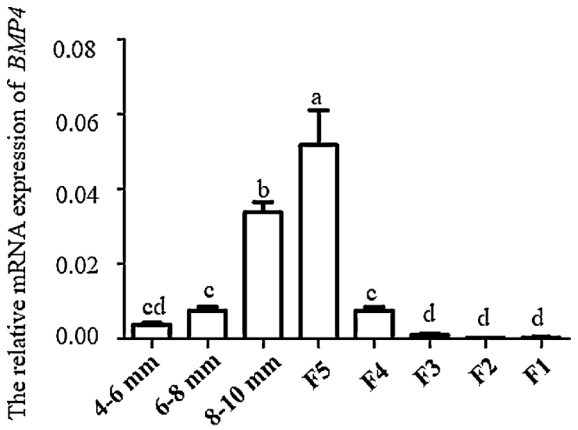

Fig. 3. Relative abundance of *BMP4* mRNA in goose granulosa layers of follicles at different developmental stages. The values for relative abundances are normalized to *18 s rRNA* and *β-actin* and are compared using the $2^{-\Delta\Delta Ct}$ method. The data are represented as the mean ± SD ($n = 3$). Different lowercase letters represent a difference in GCs among stages of follicular development ($P < 0.05$).

phosphorylation of AKT was less. Abundance of cleaved-Caspase-9 protein was greater with co-transfection of pEGFP-N1-BMP4 and LY294002, but was suppressed with pEGFP-N1-BMP4 transfection (Fig. 5A and B, $P < 0.05$). Similar to cleaved-Caspase-9, the relative abundance of cleaved-Caspase-3 protein with co-transfection of pEGFP-N1-BMP4 and LY294002 was less than that of the relevant control (Fig. 5A and B, $P < 0.05$), but there was no difference compared with the pEGFP-N1-BMP4 transfected group (Fig. 5A and B, $P < 0.05$). The abundance of CAD protein with co-transfection of pEGFP-N1-BMP4 and LY294002 was markedly greater compared with the pEGFP-N1-BMP4 transfected group (Fig. 5A and B, $P < 0.05$).

4. Discussion

There is an important role of *BMP4* in the processes of cellular proliferation, differentiation and apoptosis (Jeffery et al., 2005; Kayamori et al., 2008; Kim et al., 2013), and has previously only been widely cloned and characterized in some mammals and birds (Nilsson and Skinner, 2003; Onagbesan et al., 2003; Fatehi et al., 2005; Bertoldo et al., 2014). Furthermore, the regulatory mechanisms of *BMP4* are not well understood in the avian ovary, especially in geese. In the present study, the CDS of goose *BMP4* was initially cloned which contained 1212 nucleotides encoding 403 amino acids. The deduced amino acid sequence of goose *BMP4* was highly conserved with that from other species, particularly with that of ducks. Analysis of structure domains indicated that the goose

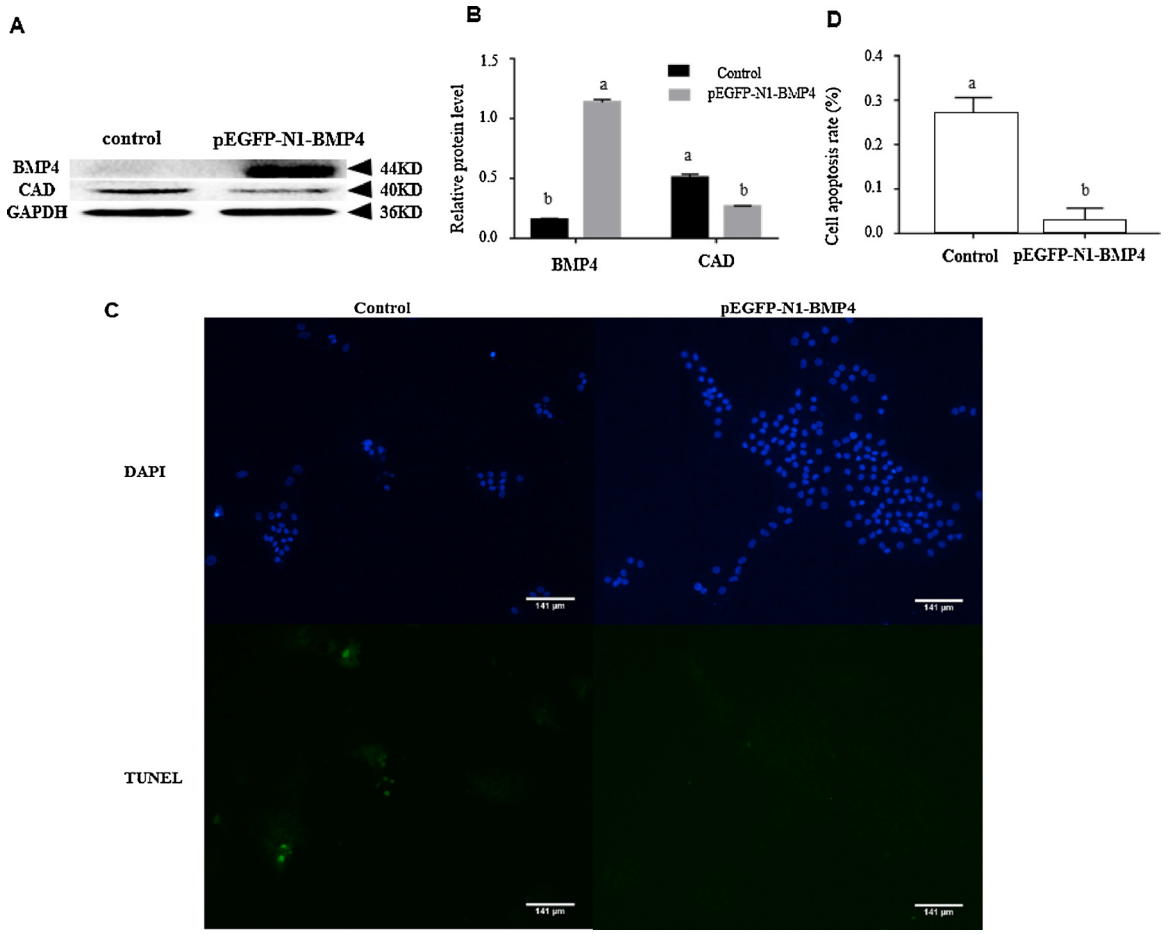

Fig. 4. Effects of transient transfection with of *BMP4* gene overexpression on apoptosis in granulosa cells of pre-hierarchical follicles. (A, B) The relative abundance of BMP4 and CAD proteins detected by western blotting and semi-quantitative analysis, respectively. The values below each western blot images represent the relative abundance of target protein compared to GAPDH. (C, D) *BMP4* gene overexpression in granulosa cells detected using the TUNEL assay method (below panel, green color), and quantification of the positive granulosa cells area and normalized against the total number of nuclei (above panel). Different lowercase letters represent a difference between bmp4 and control ($P < 0.05$). The numbers of (A) on the right side represent the molecular weight of proteins. 'Control' represents the pEGFP-N1/Lip3000 group and 'pEGFP-N1-BMP4' represents the *BMP4* gene overexpression (For interpretation of the references to colour in this figure legend, the reader is referred to the web version of this article).

BMP4 amino acid sequence was consistent with that of the BMPs family which contained one signal peptide, one TGFβ pro-peptide and one mature peptide domain (Granjeiro et al., 2005). The signal peptide was removed to form the mature peptide and the pro-peptide domain was proteolytically cleaved at a consensus Arg-X-X-Arg site to yield the carboxy-terminal mature protein (Constam and Robertson, 1999; Ducy and Karsenty, 2000; Nelsen and Christian, 2009). These results suggested that the formation of the mature terminal protein might be the reason of high homology of the mature peptide domain among different birds and mammals. Furthermore, Bragdon reported that the mature peptide domain contained seven cysteine residues that resulted in intra- or inter-molecular disulfide bonding between these residues (Bragdon et al., 2011). Six cysteine residues formed a cysteine knot and the seventh cysteine contributed to a dimerization which resulted in biological activity (Ozkaynak et al., 1990; Nohe et al., 2004). These characteristics were consistent with those of humans (Van Den Wijngaard et al., 1996), mice (Kurihara et al., 1993) and zebrafish (Hwang et al., 1997). The assessment of the phylogenetic tree indicated that goose *BMP4* was located in the same group with that of avian and mammals (Fig. 2). These results indicated that goose *BMP4* was highly conserved with that of other species, suggesting possible similar functions for avian and mammalian *BMP4*.

In the present study, relative abundances of *BMP4* mRNA increased in geese GCs as there was development of follicles from the 4 to 6 mm diameter to the F5 (largest) follicle stage, which was consistent with results of the previous study (Kim et al., 2013), and there was a lesser relatively abundance of *BMP4* in F4 - F1 follicles. In a previous study, it was documented that follicle development underwent the transition from the pre-hierarchical to pre-ovulatory stage, which was associated with the processes of follicular recruitment (< 4 mm cohorts), selection (6–8 mm cohorts) and dominance (> 9 mm cohorts) in laying hens (Johnson, 2012). The profile of relative abundances of *BMP4* mRNA during follicle development in geese indicated that *BMP4* might have a positive effect

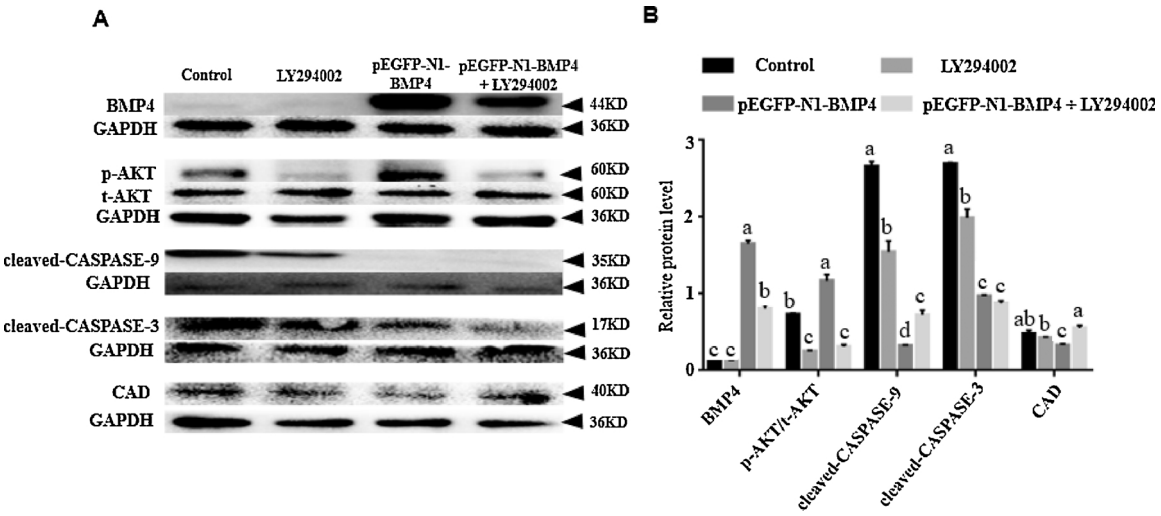

Fig. 5. Effects of LY294002 and *BMP4* gene overexpression on apoptosis in granulosa cells of pre-hierarchical follicles via the PI3K/AKT/Caspase-9 signaling pathway. (A, B) The relative abundance of proteins of the PI3K/AKT/Caspase-9 signaling pathway detected by western blotting and semi-quantitative analysis, respectively. The values below each western blot images represent the relative abundance of target the protein compared to GAPDH. Different lowercase letters represent a difference among different treatment groups ($P < 0.05$). LY294002 is an inhibitor of PI3K. The numbers of (A) on the right side represent the molecular weight of proteins. 'Control' represents the pEGFP-N1/Lip3000 group, 'LY294002' represents the LY294002 group, 'pEGFP-N1-BMP4' represents the *BMP4* gene overexpression and 'pEGFP-N1-BMP4 + LY294002' represents co-transfection of pEGFP-N1-BMP4 and LY294002.

on the survival of GCs through regulation of follicular selection. In addition, the relative abundance of *BMP4* mRNA in chickens was greater in GCs of F1 and F2 than that of F3 follicles (Onagbesan et al., 2003).However, the least abundance of *BMP4* mRNA in GCs of geese was detected in the GCs of F3-F1 follicles. The differences in the relative abundances of *BMP4* mRNA in GCs of F3 - F1 follicles in chickens compared with geese might be due to species variation. Although the follicle development is hierarchical in chickens and geese, the ovulation cycle of geese is longer than that of chickens. It was obvious that there were greater abundances of *BMP4* in GCs of F3 follicles of geese in the present study and this could inhibit apoptosis of GCs and, thus, maintain the follicle development in the hierarchy.

To investigate the effect of *BMP4* on apoptosis of GCs, the *BMP4* gene was overexpressed in the GCs of pre-hierarchical follicles *in vitro*. Results indicated that overexpression of the *BMP4* gene could result in a marked decrease in the GC apoptotic rate, indicating that the greater abundances of *BMP4* could contribute to the survival of GCs. In general, apoptotic signaling is regulated by the distinct protein families, such as the Bcl family, and the relative abundance of *bcl-2* mRNA was markedly increased after over-expression of the *BMP4* gene in the present study. The relative abundance of mRNA for apoptotic-related genes in cattle, however, did not change because of *BMP4* treatment (Kayamori et al., 2008). Thus, more experiments are needed to ascertain the regulatory mechanism through which *BMP4* inhibits apoptosis of GCs via Bcl pathway. There had been some reports that growth factors suppressed apoptosis of GCs via a mechanism other than the mitochondrial pathway (Kosaka et al., 2007; Kayamori et al., 2008; Shimizu et al., 2012). In the present study, overexpression of the *BMP4* gene resulted in a marked increase in AKT phosphorylation but there was a lesser relative abundances of *caspase-3* mRNA and cleaved-Caspase-3 and cleaved-Caspase-9 proteins. These results are consistent with those from previous studies where activation of AKT inhibited apoptosis in a variety of cells *in vitro* by regulating numerous downstream target proteins including the apoptotic initiation protein Caspase-9 (Kuida, 2000; Song et al., 2005). The activated Caspase-3 protein could cleave the CAD-ICAD complex, and CAD could induce DNA fragmentation (Lechardeur et al., 2005). The results of the present study indicated that overexpression of the *BMP4* gene resulted in a decrease in abundance of the CAD protein. These results suggested that *BMP4* might inhibit apoptosis of GCs via both the Bcl and AKT/Caspase/CAD pathways.

The PI3K/AKT signaling pathway induced by growth factors had a pivotal role in inhibiting cell apoptosis (Downward, 1998; Shiojima and Walsh, 2002), and proliferation as well as differentiation (Katso et al., 2001; Sen et al., 2003; Lechardeur et al., 2005). In the present study, the amount of AKT phosphorylation was suppressed after LY294002 treatment, which indicated that LY294002 could inhibit the promoting effect of *BMP4* gene overexpression on the amount of AKT phosphorylation. When pEGFP-N1-BMP4 and LY294002 were co-transfected into GCs, the amount of AKT phosphorylation was less compared with GCs with only pEGFP-N1-BMP4 transfection, which suggested that *BMP4* inhibited apoptosis of GCs via the PI3K/AKT signaling pathway. The abundances of the Caspase-9 and Caspase-3 proteins were less because of co-transfection compared with only LY294002 transfection but that of the Caspase-9 protein was greater compared with pEGFP-N1-BMP4 transfection, suggesting that *BMP4* might inhibit the synthesis of the Caspase-9 protein via another signaling pathway. When the combined results are considered, *BMP4* might suppress both the abundance of Caspase-9 mRNA and protein to inhibit apoptosis of GCs via the PI3K/AKT signaling pathway.

In conclusion, as a result of the present research the intact CDS of goose *BMP4* was obtained which encoded for 403 amino acids consisting of one signal peptide, one TGFβ pro-peptide and one mature peptide domain. Relative abundances of *BMP4* mRNA in GCs

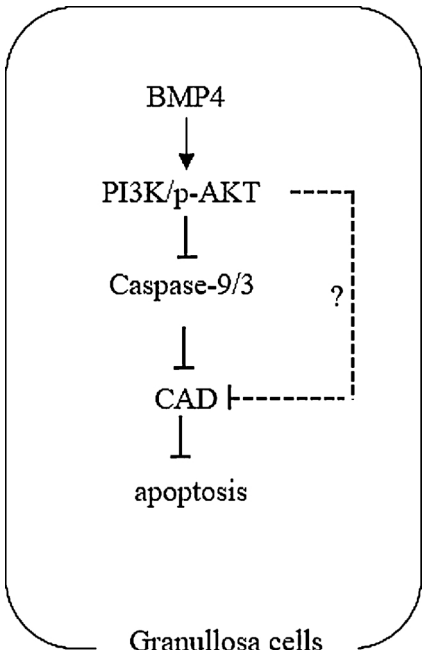

Fig. 6. Schema of the inhibitory mechanism of *BMP4* in granulosa cell apoptosis. The inhibitory action of *BMP4* is not only associated with the mitochondrial pathway but also with PI3K/AKT signaling pathway. *BMP4* might inhibit the CAD via PI3K/AKT/Caspase signaling pathway to suppress the granulosa cell apoptosis. In addition, *BMP4* might also directly inhibit CAD protein synthesis leading to suppression of granulosa cell apoptosis. '→' represents the promotion. '┤'represents the inhibitory. '————— 'represents the unknown signaling pathway. '?' indicates unknown factors.

increased during the development of follicles and reached the maximum in the F5 follicle. At the cellular level, overexpression of the *BMP4* gene resulted in a marked suppression of apoptosis in GCs. The *BMP4* protein, therefore, might not only regulate the abundance of *bcl-2* and *caspase* family mRNAs, but also might directly inhibit synthesis of the CAD protein suppressing apoptosis of GCs *in vitro* (Fig. 6). These results suggest that *BMP4* inhibits apoptosis of GCs via PI3K/AKT/Caspase-9 signaling pathway.

Declaration of interest

The author declare no conflict of interest regarding the publication of this article.

Acknowledgments

This research was supported by the National Natural Science Funds of China [grant numbers 31672424]; the Ministry of Agriculture of the People's Republic of China [grant numbers CARS-42-4]; and the Ministry of Science and Technology of the People's Republic of China (MOST) [grant numbers 2015BAD03B06].

Appendix A. Supplementary data

Supplementary material related to this article can be found, in the online version, at doi:https://doi.org/10.1016/j.anireprosci.2018.11.014.

References

Bertoldo, M.J., Duffard, N., Bernard, J., Frapsauce, C., Calais, L., Rico, C., Mermillod, P., Locatelli, Y., 2014. Effects of bone morphogenetic protein 4 (BMP4) supplementation during culture of the sheep ovarian cortex. Anim. Reprod. Sci. 149, 124–134. https://doi.org/10.1016/j.anireprosci.2014.07.010.

Bragdon, B., Moseychuk, O., Saldanha, S., King, D., Julian, J., Nohe, A., 2011. Bone morphogenetic proteins: a critical review. Cell Signal. 23, 609–620. https://doi.org/10.1016/j.cellsig.2010.10.003.

Constam, D.B., Robertson, E.J., 1999. Regulation of bone morphogenetic protein activity by pro domains and proprotein convertases. J. Cell Biol. 144, 139–149 PMC2148113.

Da, C.E., De Souza, G.B., Passos, J.R., Silva, A.W., Dau, A.M., Saraiva, M.V., Lobo, R.N., Silva, J.R., 2017. Effects of bone morphogenetic protein 4 (BMP4) on in vitro development and survival of bovine preantral follicles enclosed in fragments ovarian tissue. Zygote 25, 256–264. https://doi.org/10.1017/S0967199417000089.

Deng, Y., Gan, X., Chen, D., Huang, H.L., Yuan, J.S., Qiu, J.M., Hu, S.Q., Hu, J.W., Wang, J.W., 2018. Comparison of growth characteristics of in vitro cultured granulosa cells from geese follicles at different developmental stages. Biosci. Rep. 38https://doi.org/10.1042/BSR20171361. BSR20171361.

Ding, X., Zhang, X., Mu, Y., Li, Y., Hao, J., 2013. Effects of BMP4/SMAD signaling pathway on mouse primordial follicle growth and survival via up-regulation of Sohlh2 and c-kit. Mol. Reprod. Dev. 80, 70–78. https://doi.org/10.1002/mrd.22138.

Downward, J., 1998. Mechanisms and consequences of activation of protein kinase B/Akt. Curr. Opin. Cell Biol. 10, 262–267 PMID: 9561851.
Drummond, A.E., 2005. TGFbeta signalling in the development of ovarian function. Cell Tissue Res. 322, 107–115. https://doi.org/10.1007/s00441-005-1153-1.
Ducy, P., Karsenty, G., 2000. The family of bone morphogenetic proteins. Kidney Int. 57, 2207–2214. https://doi.org/10.1046/j.1523-1755.2000.00081.x.
Fatehi, A.N., Van, D.H.R., Colenbrander, B., Daemen, A.J., Van Tol, H.T., Monteiro, R.M., Roelen, B.A., Bevers, M.M., 2005. Expression of bone morphogenetic protein2 (BMP2), BMP4 and BMP receptors in the bovine ovary but absence of effects of BMP2 and BMP4 during IVM on bovine oocyte nuclear maturation and subsequent embryo development. Theriogenology. 63, 872–889. https://doi.org/10.1016/j.theriogenology.2004.05.013.
Gavrieli, Y., Sherman, Y., Bensasson, S.A., 1992. Identification of programmed cell death in situ via specific labeling of nuclear DNA fragmentation. J. Cell Biol. 119, 493–501 PMCID: PMC2289665.
Granjeiro, J.M., Oliveira, R.C., Bustos-Valenzuela, J.C., Sogayar, M.C., Taga, R., 2005. Bone morphogenetic proteins: from structure to clinical use. Braz. J. Med. Biol. Res. 38, 1463–1473. http://doi.org//S0100-879X2005001000003.
Hwang, S.P., Tsou, M.F., Lin, Y.C., Liu, C.H., 1997. The zebrafish BMP4 gene: sequence analysis and expression pattern during embryonic development. DNA Cell Biol. 16, 1003–1011. https://doi.org/10.1089/dna.1997.16.1003.
Inoue, N., Matsuda, F., Goto, Y., Manabe, N., 2011. Role of cell-death ligand-receptor system of granulosa cells in selective follicular atresia in porcine ovary. J. Reprod. Dev. 57, 169–175 PMID: 21551974.
Jeffery, T.K., Upton, P.D., Trembath, R.C., Morrell, N.W., 2005. BMP4 inhibits proliferation and promotes myocyte differentiation of lung fibroblasts via Smad1 and JNK pathways. Am. J. Physiol. Lung Cell Mol. Physiol. 288, 370–378. https://doi.org/10.1152/ajplung.00242.2004.
Johnson, A.L., 2003. Intracellular mechanisms regulating cell survival in ovarian follicles. Anim. Reprod. Sci. 78, 185–201 PMID: 12818644.
Johnson, P.A., 2012. Follicle selection in the avian ovary. Reprod. Domest. Anim. 47 (Suppl 4), 283–287. https://doi.org/10.1111/j.1439-0531.2012.02087.x.
Katso, R., Okkenhaug, K., Ahmadi, K., White, S., Timms, J., Waterfield, M.D., 2001. Cellular function of phosphoinositide 3-kinases: implications for development, homeostasis, and cancer. Annu. Rev. Cell Dev. Biol. 17, 615–675. https://doi.org/10.1146/annurev.cellbio.17.1.615.
Kayamori, T., Kosaka, N., Miyamoto, A., Shimizu, T., 2008. The differential pathways of bone morphogenetic protein (BMP)-4 and -7 in the suppression of the bovine granulosa cell apoptosis. Mol. Cell Biochem. 323, 161–168. https://doi.org/10.1007/s11010-008-9976-1.
Kim, D., Ocón-Grove, O., Johnson, A.L., 2013. Bone morphogenetic protein 4 supports the initial differentiation of hen (Gallus gallus) granulosa cells. Biol. Reprod. 88, 161. https://doi.org/10.1095/biolreprod.113.109694.
Knight, P.G., Glister, C., 2006. TGF-beta superfamily members and ovarian follicle development. Reproduction. 132, 191–206.
Koinuma, D., Imamura, T., Miyazono, K., 2005. [TGF-beta family (TGF-beta, activin, BMP)]. Nihon Rinsho 63 (Suppl 4), 215–219 PMID: 15861659.
Kosaka, N., Sudo, N., Miyamoto, A., Shimizu, T., 2007. Vascular endothelial growth factor (VEGF) suppresses ovarian granulosa cell apoptosis in vitro. Biochem. Biophys. Res. Commun. 363, 733–737. https://doi.org/10.1016/j.bbrc.2007.09.061.
Kuida, K., 2000. Caspase-9. Int. J. Biochem. Cell Biol. 32, 121–124 PMID: 10687948.
Kurihara, T., Kitamura, K., Takaoka, K., Nakazato, H., 1993. Murine bone morphogenetic protein-4 gene: existence of multiple promoters and exons for the 5'-untranslated region. Biochem. Biophys. Res. Commun. 192, 1049–1056. https://doi.org/10.1006/bbrc.1993.1523.
Lechardeur, D., Dougaparsad, S., Nemes, C., Lukacs, G.L., 2005. Oligomerization state of the DNA fragmentation factor in normal and apoptotic cells. J. Biol. Chem. 280, 40216–40225. https://doi.org/10.1074/jbc.M502220200.
Livak, K.J., Schmittgen, T.D., 2001. Analysis of relative gene expression data using real-time quantitative PCR and the 2 $-\Delta\Delta$ C t method. Methods 25, 402–408. https://doi.org/10.1006/meth.2001.1262.
Nelsen, S.M., Christian, J.L., 2009. Site-specific cleavage of BMP4 by Furin, PC6, and PC7. J. Biol. Chem. 284, 27157–27166. https://doi.org/10.1074/jbc.M109.028506.
Nilsson, E.E., Skinner, M.K., 2003. Bone morphogenetic Protein-4 acts as an ovarian follicle survival factor and promotes primordial follicle Development1. Biol. Reprod. 69, 1265–1272. https://doi.org/10.1095/biolreprod.103.018671.
Nohe, A., Keating, E., Knaus, P., Petersen, N.O., 2004. Signal transduction of bone morphogenetic protein receptors. Cell Signal. 16, 291–299 PMID: 14687659.
Onagbesan, O.M., Bruggeman, V., Van, A.P., Tona, K., Williams, J., Decuypere, E., 2003. BMPs and BMPRs in chicken ovary and effects of BMP-4 and -7 on granulosa cell proliferation and progesterone production in vitro. Am. J. Physiol. Endocrinol. Metab. 285, E973–E983. https://doi.org/10.1152/ajpendo.00104.2003.
Ozkaynak, E., Rueger, D.C., Drier, E.A., Corbett, C., Ridge, R.J., Sampath, T.K., Oppermann, H., 1990. OP-1 cDNA encodes an osteogenic protein in the TGF-beta family. EMBO J. 9, 2085–2093 PMCID: PMC551926.
Sen, P., Mukherjee, S., Ray, D., Raha, S., 2003. Involvement of the Akt/PKB signaling pathway with disease processes. Mol. Cell Biochem. 253, 241–246 PMID: 14619975.
Shapiro, S.S., Wilk, M.B., 1965. An analysis of variance test for normality (Complete Samples). Biometrika 52, 591–611. http://www.jstor.org/stable/2333709.
Shi, Y., Massague, J., 2003. Mechanisms of TGF-beta signaling from cell membrane to the nucleus. Cell 113, 685–700 PMID: 12809600.
Shimasaki, S., Moore, R.K., Otsuka, F., Erickson, G.F., 2004. The bone morphogenetic protein system in mammalian reproduction. Endocr. Rev. 25, 72–101. https://doi.org/10.1210/er.2003-0007.
Shimasaki, S., Zachow, R.J., Li, D., Kim, H., Iemura, S., Ueno, N., Sampath, K., Chang, R.J., Erickson, G.F., 1999. A functional bone morphogenetic protein system in the ovary. Proc. Natl. Acad. Sci. U. S. A. 96, 7282–7287 PMID: 10377406.
Shimizu, T., Kayamori, T., Murayama, C., Miyamoto, A., 2012. Bone morphogenetic protein (BMP)-4 and BMP-7 suppress granulosa cell apoptosis via different pathways: BMP-4 via PI3K/PDK-1/Akt and BMP-7 via PI3K/PDK-1/PKC. Biochem. Biophys. Res. Commun. 417, 869–873. https://doi.org/10.1016/j.bbrc.2011.12.064.
Shiojima, I., Walsh, K., 2002. Role of Akt signaling in vascular homeostasis and angiogenesis. Circ. Res. 90, 1243–1250 PMID: 12089061.
Song, G., Ouyang, G., Bao, S., 2005. The activation of Akt/PKB signaling pathway and cell survival. J. Cell. Mol. Med. 9, 59–71 PMID: 15784165.
Tilly, J.L., Kowalski, K.I., Johnson, A.L., Hsueh, A.J.W., 1991. Involvement of apoptosis in ovarian follicular atresia and postovulatory regression. Endocrine 129, 2799–2801. https://doi.org/10.1210/endo-129-5-2799.
Van Den Wijngaard, A., Van Kraay, M., Van Zoelen, E.J., Olijve, W., Boersma, C.J., 1996. Genomic organization of the human bone morphogenetic protein-4 gene: molecular basis for multiple transcripts. Biochem. Biophys. Res. Commun. 219, 789–794. https://doi.org/10.1006/bbrc.1996.0312.
Wei, Q., Zhu, G., Cui, X., Kang, L., Cao, D., Jiang, Y., 2013. Expression of CCT6A mRNA in chicken granulosa cells is regulated by progesterone. Gen. Comp. Endocrinol. 189, 15–23. https://doi.org/10.1016/j.ygcen.2013.04.019.
Wu, J., Wong, A.C.M., 2003. A note on determining the p-Value of Bartlett"s test of homogeneity of variances. Commun. Stat. Theory Methods 32, 91–101. https://doi.org/10.1081/STA-120017801.
Zhang, X., Zhang, H., Gao, Q., Ji, S., Bing, L., Jing, H., 2015. Sohlh2 inhibits the apoptosis of mouse primordial follicle oocytes via C-kit/PI3K/Akt/Foxo3a signalling pathway. Reprod. Biomed. Online 30, 514–521. https://doi.org/10.1016/j.rbmo.2015.01.015.